Electronic Supplementary Material (ESI) for Analyst.

Supplementary information for:

Long-stem shaped multifunctional molecular beacon for highly sensitive nucleic acids determination via intramolecular and intermolecular interactions based strand displacement amplification

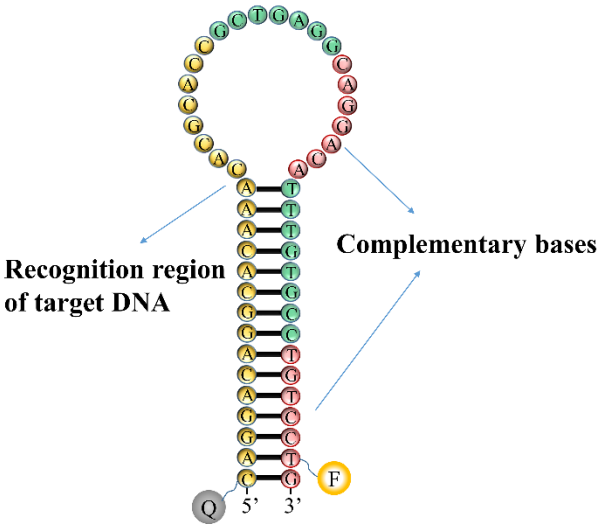

Scheme S1. Schematic diagram of LS-MMB. The fragment shown in yellow indicates the recognition region of target gene, while the two fragments shown in red are complementary to each other to facilitate the SDA.

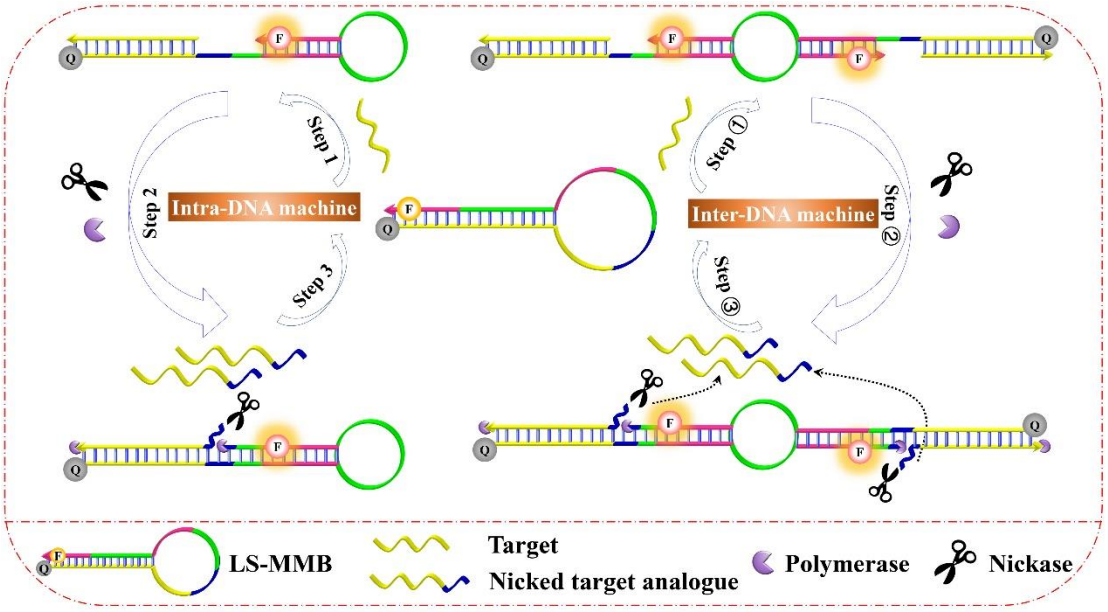

Scheme S2. Imaginary graph of LS-MMB based molecular machine. The presence of target gene would activate the DNA machine based on autonomously performed polymerization, nicking, and strand displacement procedures, enabling extensively accumulation of nicked fragments that have similar bases as target DNA for further hybridization with residual LS-MMB molecules. We suggest it as a possible route to amplify DNA detection. The nickase recognition site is presented in blue.

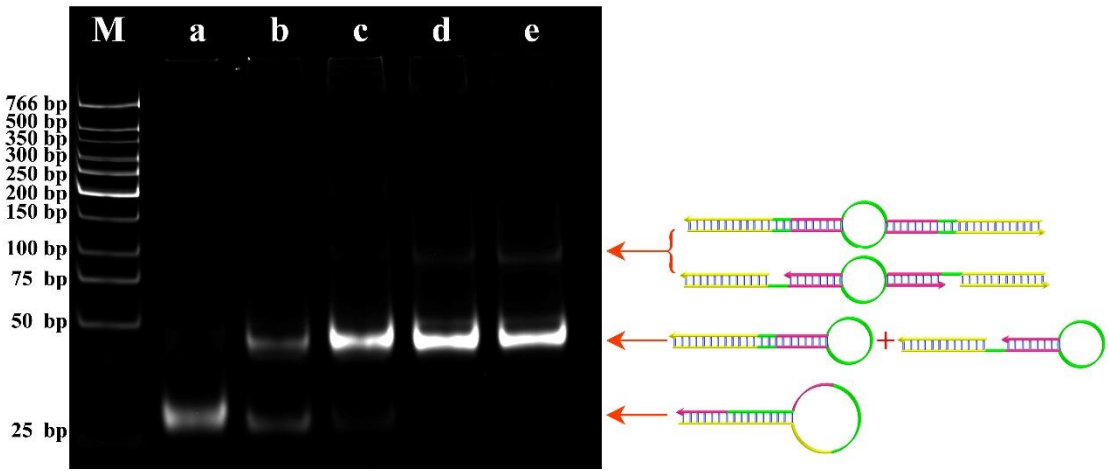

Figure S1. Gel electrophoresis analysis of label-free LS-MMB (320 nM) based SDA system in the absence (a) and presence of 40 nM (b), 80 nM (c), 160 nM (d), and 320 nM (e) target gene, respectively. "M" is the abbreviation of "DNA Marker".

Mechanism demonstration by gel electrophoresis

For clearly explanation of the LS-MMB based SDA, 12 % native PAGE analysis was conducted in priority to verify the expected signal transition mechanism. As provided in **Figure S1**, even coexisted with polymerase, only one band of LS-MMB was appeared in lane a, indicating that the LS-MMB was tightly locked by the long stem so that no any other background bands were observed. After adding one-eighth (lane b) or one quarter (lane c) dosage target DNA, the band of LS-MMB was decreased, and a new band with lower mobility and high molecular weight appeared above. Definitely, the newly formed band indicates the mixture of LS-MMB/Target complex and intramolecular extended LS-MMB. They are not separated from each other because of their similar configuration and bases number, as well as limited electrophoretic resolution. Surprisingly, after further increase the dosage of target, the band represented

LS-MMB was completely exhausted and replaced by two bands in the presence of half-dosage target (lane d) and equal amount target (lane e). The lower band have a same mobile position to the upper band shown in lane b and lane c, while the upper band with a slow migration rate was presumably in agreement with the location of two LS-MMB/Target complex formed dimer or extended LS-MMB composed dimer by intermolecular interaction. Likewise, the two dimers shown an identical position because of the aforementioned same reasons. Evidently, these results demonstrate that two different SDA are involved in the sensing system, and its sensing capability for gene detection is also been indirectly validated in view of the band of LS-MMB presents a trend of decreasing from lane b to lane d that could be related to the presence and concentration of targets.

Table S1. Detailed comparison of the assay performance for gene analysis by the current study with literature reports.

Method	Detection limit	Linear range	Single-base mutation response (%)	Category	Ref
Integration of intermolecular G-quadruplex structure with sticky-end pairing	200 pM	400 pM to 50 nM	58 %	Colorimetric assay	[1]
Templated chemistry	200 pM	200 pM to 10 nM	About 65 %	Fluorescent assay	[2]
Fluorescence near gold nanoparticles	100 pM	100 pM to 1 nM	No evaluation	Fluorescent assay	[3]
Cascade DNA nanomachine and exponential amplification	50 pM	50 pM to 150 nM	78 %	Fluorescent assay	[4]
Nicking endonuclease-assisted fluorescence resonance energy transfer	77 pM	100 pM to 50 nM	About 180 %	Fluorescent assay	[5]
Two fluorophores tagged MB	170 pM	1000 pM to 1000 nM	No evaluation	Fluorescent assay	[6]
Dendritic DNA/PNA Assembly	100 fM	0.1 pM to 10 nM	About 64 %	Electrochemical assay	[7]
In situ hybridization chain reaction amplification	15 fM	25 fM to 100 pM	About 33 %	Electrochemical assay	[8]
LS-MMB based SDA	50 pM	50 pM to 160 nM	43.9 %	Fluorescent assay	Present study

Reference

[1] H. Li, Z.S. Wu, Z. Shen, G. Shen, R. Yu, Architecture based on the integration of intermolecular G-quadruplex structure with sticky-end pairing and colorimetric detection of DNA hybridization, Nanoscale 6(4) (2013) 2218.

[2] E.M. Harcourt, E.T. Kool, Amplified microRNA detection by templated chemistry, Nucleic Acids Research 40(9) (2012) e65.

[3] Y. Cheng, T. Stakenborg, D.P. Van, L. Lagae, M. Wang, H. Chen, G. Borghs, Fluorescence near gold nanoparticles for DNA sensing, Analytical Chemistry 83(4) (2016) 1307-1314.

[4] J. Xu, Z.S. Wu, W. Shen, H. Xu, H. Li, L. Jia, Cascade DNA nanomachine and exponential amplification biosensing, Biosensors & Bioelectronics 73 (2015) 19.

[5] L. Xu, Y. Zhu, W. Ma, H. Kuang, L. Liu, L. Wang, C. Xu, Sensitive and Specific DNA Detection Based on Nicking Endonuclease-Assisted Fluorescence Resonance Energy Transfer Amplification, Journal of Physical Chemistry C 115(33) (2011).

[6] P. Zhang, T. Beck, W. Tan, Design of a molecular beacon DNA probe with two fluorophores, Angewandte Chemie 113(2) (2001) 416-419.

[7] F. Xuan, T.W. Fan, I.-M. Hsing, Electrochemical interrogation of kinetically-controlled dendritic DNA/PNA assembly for immobilization-free and enzyme-free nucleic acids sensing, ACS nano 9(5) (2015) 5027-5033.

[8] Y. Chen, J. Xu, J. Su, Y. Xiang, R. Yuan, Y. Chai, In situ hybridization chain reaction amplification for universal and highly sensitive electrochemiluminescent detection of DNA, Analytical chemistry 84(18) (2012) 7750-7755.